Radiology

Detection of Colorectal Hepatic Metastases Is Superior at Standard Radiation Dose CT versus Reduced Dose CT

Corey T. Jensen, MD • Nicolaus A. Wagner-Bartak, MD • Lan N. Vu, MD • Xinming Liu, PhD • Bharat Raval, MD • David Martinez, RT (R) (CT) • Wei Wei, MS • Yuan Cheng, PhD • Ehsan Samei, PhD • Shiva Gupta, MD

From the Departments of Diagnostic Radiology (C.T.J., N.A.W., L.N.V., B.R., D.M., S.G.), Biostatistics (W.W.), and Physics (X.L.), University of Texas MD Anderson Cancer Center, 1400 Pressler St, Unit 1473, Houston, TX 77030-4009; and Duke University Medical Center, Durham, NC (Y.C., E.S.). Received July 14, 2018; revision requested August 20; final revision received September 18; accepted October 8. **Address correspondence to** C.T.J. (e-mail: *cjensen@mdanderson.org*).

Supported by an institutional Cancer Center Support Grant from the National Institutes of Health/National Cancer Institute under award number P30CA016672 NCI-2018-01272/NCT03151564.

Conflicts of interest are listed at the end of this article.

Radiology 2019; 290:400–409 • https://doi.org/10.1148/radiol.2018181657 • Content codes: CT GI SQ

Purpose: To evaluate colorectal cancer hepatic metastasis detection and characterization between reduced radiation dose (RD) and standard dose (SD) contrast material–enhanced CT of the abdomen and to qualitatively compare between filtered back projection (FBP) and iterative reconstruction algorithms.

Materials and Methods: In this prospective study (from May 2017 through November 2017), 52 adults with biopsy-proven colorectal cancer and suspected hepatic metastases at baseline CT underwent two portal venous phase CT scans: SD and RD in the same breath hold. Three radiologists, blinded to examination details, performed detection and characterization of 2–15-mm lesions on the SD FBP and RD adaptive statistical iterative reconstruction (ASIR)–V 60% series images. Readers assessed overall image quality and lesions between SD FBP and seven different iterative reconstructions. Two nonblinded consensus reviewers established the reference standard using the picture archiving and communication system lesion marks of each reader, multiple comparison examinations, and clinical data.

Results: RD CT resulted in a mean dose reduction of 54% compared with SD. Of the 260 lesions (233 metastatic, 27 benign), 212 (82%; 95% confidence interval [CI]: 76%, 86%) were detected with RD CT, whereas 252 (97%; 95% CI: 94%, 99%) were detected with SD ($P < .001$); per-lesion sensitivity was 79% (95% CI: 74%, 84%) and 94% (95% CI: 90%, 96%) ($P < .001$), respectively. Mean qualitative scores ranked SD images as higher quality than RD series images, and ASIR-V ranked higher than ASIR and Veo 3.0.

Conclusion: CT evaluation of colorectal liver metastases is compromised with modest radiation dose reduction, and the use of iterative reconstructions could not maintain observer performance.

CT is the main imaging modality used for oncologic assessments (1). In more recent years, concerns regarding the associated radiation exposure have spurred fears about potential risk of radiation-induced malignancy and resulted in a reduction in CT utilization (2,3). These concerns have led to a concerted effort to reduce and monitor radiation doses in CT imaging. CT manufacturers have sought methods of maintaining image quality while lowering radiation doses (4).

Filtered back projection (FBP) is the standard reconstruction for CT, however, it delivers suboptimal image quality when reduced radiation doses are used. CT manufacturers have sought methods of maintaining image quality while lowering radiation doses. One such method is iterative reconstruction (IR). IR uses known CT system characteristics to approximate an expected image. IR algorithms can significantly reduce image noise and artifacts to preserve image quality when reduced radiation doses are used, when scanning large patients, or when performing small-field-of-view studies (5). IR methods can operate in the image and/or projection space with reported moderate radiation dose reduction potential in the range of 25%–40% (4,6–8). While robust image noise reduction can be obtained with these algorithms, there is an associated degradation of resolution and variable degrees of altered image texture have been reported (9,10). A desired balance between resolution, noise, and image texture can be targeted through choosing the degree of blending of IR with FBP.

Model-based IR (MBIR) represents a more advanced and complex version of IR, using both backward and forward projections. Complex system modeling is used iteratively to varying degrees between the projection data space and image data space. MBIR algorithms include Veo (GE Healthcare, Waukesha, Wis), forward-projected MBIR solution (FIRST; Toshiba Medical Systems, Tokyo, Japan), iterative model reconstruction (IMR; Philips Medical Systems, Best, the Netherlands), and advanced model-based IR (ADMIRE; Siemens Healthcare, Forchheim, Germany) (11). MBIR provides robust noise reduction, but requires significantly longer reconstruction time and has been criticized for having a greater degree of altered image texture (12–17).

Abbreviations

ASIR = adaptive statistical IR, CI = confidence interval, CNR = contrast-to-noise ratio, $CTDI_{vol}$ = volume CT dose index, DLP = dose length product, FBP = filtered back projection, IR = iterative reconstruction, LCLA = low contrast low attenuation, MBIR = model-based IR, OR = odds ratio, RD = reduced dose, SD = standard dose, SSDE = size-specific dose index

Summary

CT of low-contrast liver lesions is compromised by modest radiation dose reduction. The use of iterative reconstructions could not maintain observer performance.

Implications for Patient Care

- For small, low-contrast liver lesions, CT radiation dose levels suggested by the American College of Radiology dose index registry may be too low for adequate detection.
- Low-to-moderate levels of iterative reconstruction strength qualitatively improved both reduced radiation dose and standard dose CT scans.

Adaptive statistical IR (ASIR)–V (GE Healthcare) is a new version of a vendor-specific IR. ASIR-V is essentially a hybrid of ASIR and Veo reconstruction methods using a less-complex model than MBIR that de-emphasizes system optics, thus allowing for much faster image reconstruction (18). However, compared with ASIR, ASIR-V provides improved noise, object, and physics modeling. ASIR-V has been shown to reduce noise and improve image quality in the abdomen when compared with ASIR (19,20). Kwon et al (21) indicated the potential for an additional radiation dose reduction of 35% in the abdomen with ASIR-V when compared with ASIR. However, concerns have been raised regarding limitations in task-specific diagnoses as radiation dose levels are reduced (22–26).

The oncologic evaluation of low-contrast lesions, particularly in the liver, is one such challenging clinical scenario that requires further evaluation in the setting of radiation dose reduction. Recent reports indicate that the degree of potential radiation reduction available with IR methods compared with FBP may be less than initially expected (9,10). This discordance with prior studies is in part due to varying study designs that are necessarily limited by the amount of radiation dose delivered to patients and a limited capacity of observer studies to assess the various combinations of radiation levels and reconstruction methods (23,27). Many phantom studies are difficult to translate to practice, as nonlinear IR methods provide varying results when actual patients of differing body sizes and shapes are scanned (11,28). Additionally, a few studies lack direct comparison to a reference standard and others have relied only on qualitative image assessment and the assessment of image characteristics rather than performance related to a specific clinical task.

The purpose of this study was to prospectively evaluate the detection (ie, visibility) of colorectal cancer hepatic metastases, lesion characterization, and false-positive markings between reduced dose (RD) and standard dose (SD) contrast material–enhanced CT of the abdomen in the same breath hold and to qualitatively compare lesions between FBP, ASIR, ASIR-V, and Veo 3.0 reconstruction algorithms.

Materials and Methods

This prospective study (NCI-2018–01272) was approved by our institutional review board as Health Insurance Portability and Accountability Act compliant, and informed consent was obtained.

Participant Population

On the basis of expected CT accuracy with an assumed discordant rate of 10% or higher, our power analysis indicated that 52 participants would provide a power of at least 80% with a one-sided type I error rate of 10%. We scanned patients between May 2017 and November 2017 using a convenience sample with inclusion and exclusion criteria listed in Figure 1. Each patient's age, sex, height, weight, and body mass index were recorded. Additionally, the total number of contrast-enhanced CT examinations performed within 6 months, before or after the study examination, were tabulated; the number of days since the most recent prior CT examination was also calculated.

Radiation Dose Estimation

The effective diameter of each patient was obtained based on the anteroposterior and lateral scout measurements (effective diameter = [anteroposterior diameter times lateral diameter]$^{1/2}$). The volume CT dose index ($CTDI_{vol}$) for a 32-cm phantom and the dose length product (DLP) were obtained. Size-specific dose estimates (SSDEs) were calculated as recommended by the American Association of Physicists in Medicine report number 204 (29,30).

Imaging Technique and Postprocessing

All patients underwent CT of the abdomen performed by using the same imaging protocol (Table 1). The tube current parameters for the RD scan were set to approximate a 50% radiation dose reduction. The SD scan was performed in the craniocaudal direction, and the RD scan was performed without interval delay in the reverse direction during the same breath hold. This target reduction was chosen to approximate the 25th–75th percentile $CTDI_{vol}$ reported by sites in the Dose Index Registry of the American College of Radiology for contrast-enhanced CT of the chest, abdomen, and pelvis ($CTDI_{vol}$, 9–19 mGy) (31). One hundred twenty-five to 150 mL of low osmolar iohexol 350 mg I/mL (Omnipaque 350, GE Healthcare) was injected at 3–4 mL/sec, the former given to smaller patients (digital field of view [DFOV], 40 cm or lower) and the latter given to larger patients (DFOV, 41 cm or higher). Bolus tracking was used, with a 100-HU trigger value in the abdominal aorta at the level of the celiac artery with a scan delay of 46 seconds.

Eight axial reconstructions were performed for each patient to a 2.5-mm section thickness: four at standard radiation doses (SD) (FBP, ASIR 80% [A80], ASIR-V 30% [AV30], ASIR-V 60% [AV60]) and four at reduced radiation doses (RD) (Veo 3.0, ASIR 80% [A80], ASIR-V 30% [AV30], ASIR-V 60% [AV60]). The Veo 3.0 reconstruction utilized a 5% noise reduction preset with 1.25-mm section optimization and texture feature active, as suggested in prior publications

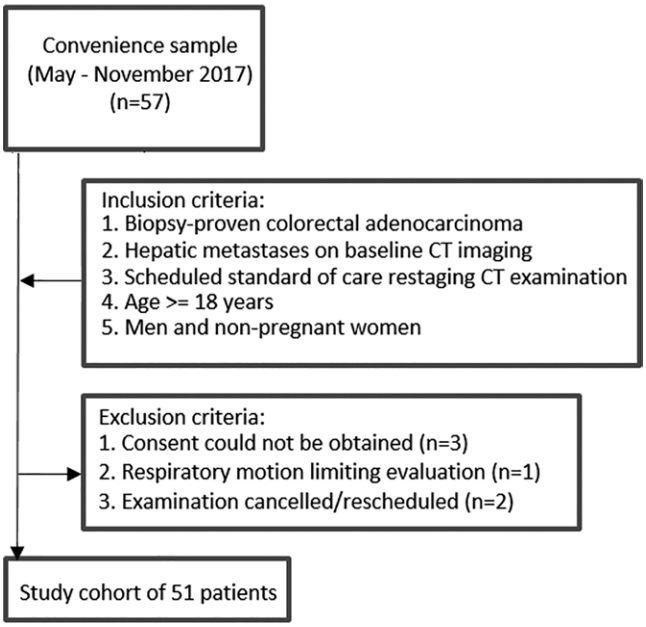

Figure 1: Flowchart of participant accrual.

Table 1: Imaging Settings for the Abdominal CT Protocol

Parameter	Datum
Scanner model	Discovery CT750 HD
Scan mode	Helical, single source
Detector configuration (mm)	64 × 0.6
Beam collimation (mm)	40
Pitch	0.5
Rotation time (sec)	0.5
Table speed (mm/rotation)	20
Tube current modulation (noise index/minimum mA)	
SD scan	12/250
RD scan	19/125
Tube potential (kV)	120
Section thickness (mm)	5
Reconstruction thickness and increment (mm)	2.5/2.5
Reconstruction algorithm	
FBP	Standard
ASIR 80%	Iterative (image space)
Veo 3.0	Iterative (projection data space)
ASIR-V 30%/60%	Iterative (hybrid; deemphasizes system optics compared with Veo)
Reconstruction kernel	Standard plus

Note.—ASIR = adaptive statistical iterative reconstruction, FBP = filtered back projection, RD = reduced dose, SD = standard dose.

(15,16). RD FBP has been previously shown to have inferior diagnostic performance and thus was not chosen for evaluation in this study (27). The single 80% blend of ASIR allowed for matching results to a prior retrospective evaluation and provided a degree of noise reduction between AV30 and AV60 (14). The utility of MBIR has been demonstrated only in dose reduction settings, and the prior retrospective study by Goodenberger et al (14) showed Veo 3.0 to be inferior to ASIR-V; therefore, a standard dose Veo reconstruction was not assessed. All images were reviewed in standard clinical conditions with high-resolution monitors by using a two-monitor picture archiving and communications system.

Lesion Detection and Reference Standard

Three board-certified abdominal radiologists independently performed lesion detection in two primary series while blinded to all information except cancer diagnosis. Two readers were fellowship trained in abdominal imaging and had 8 years (N.A.W.) and 6 years (S.G.) of additional experience reading abdominal CT studies. The third reader (B.R.) had more than 25 years of experience in the subspecialty reading of abdominal CT studies. Images in 51 participants were assessed over four sessions, for a total review of 102 scans: SD FBP versus RD AV60. Only noncalcified, hypoattenuating lesions measuring 0.2–1.5 cm were to be marked as lesions; the primary aim was to assess small (<0.6 cm) lesion detection, but we have noted that even some larger lesions are difficult to detect in practice. Thus, we included two additional subsets of equal lesion size range (0.6–1.0 cm and 1.0–1.5 cm). Peritoneal and hepatic capsular lesions were to be ignored by readers. In the setting of conglomerate lesions, lesions were counted separately only if there was intervening normal hepatic parenchyma. Likert-type scores were given for each lesion with respect to characterization (a score of 1 indicated definitely benign; 2, likely benign; 3, malignancy not excluded; 4, likely malignant; 5, definitely malignant) and related confidence in the diagnosis (1 for low confidence up to 5 for high confidence). Reconstructions were presented in a randomized fashion, and review of the SD FBP versus RD AV60 images in the same participant was separated by a delay period of 3 weeks to minimize recall. There was no time limit for review, but it was suggested that the radiologists read in a manner similar to clinical practice, which included the ability to review coronal and sagittal reconstructions.

Two nonblinded consensus reviewers (fellowship-trained abdominal radiologists with 7 years [C.T.J.] and 8 years [N.A.W.] in practice) subsequently established the reference standard using the saved reader marks (on both the SD and RD series) and all available clinical data. Comparison was made to all available cross-sectional imaging examinations (CT, MRI, and PET/CT). All lesions identified were measured and classified by the consensus reviewers as metastatic or benign, and false reader lesion marks were also recorded. For participants with 20 or more metastatic lesions identified with the reference standard, lesion detection performance was not assessed. For performance metrics, benign lesions scored as 3 or higher on the malignancy scale were considered false-positive results against the reference standard. Malignant lesions according to the reference standard that were either not identified by reviewers or that scored 2 or lower on the malignancy scale were considered false-negative results (11).

Qualitative Analysis

After each primary series underwent lesion detection, readers scored the series for overall image quality with respect to artifacts, image texture, and qualitative resolution (where a score of 1 indicated excellent image quality without related issues of concern; 2, minor issues not interfering with diagnostic decision making; 3, minor issues possibly interfering with diagnostic decision making; 4, major issues affecting visualization of major structures but diagnosis still possible; and 5, issues affecting diagnostic information).

For each participant, after the second lesion detection session was completed and primary image quality score was given, all eight reconstructions for that participant were displayed side-by-side. The hanging order of the reconstructions was randomized, and annotations were removed. The view ports were linked so that identical section levels could be evaluated on all reconstructions while scrolling through the images. The scans were initially presented with a window width/level setting of 500/50 HU, and the readers were allowed to scroll through the cases, change the window width/level settings, zoom, and pan while reviewing the cases. A comparative scale was used to rank overall lesion depiction (eg, margin sharpness and lesion conspicuity) and image quality (eg, qualitative image resolution, soft-tissue contrast, noise, image texture) in the abdomen for each reconstruction. A rank of 0 was given for the best series, −1 for slightly inferior (no influence on diagnosis), −2 for mildly inferior (possible influence on diagnosis), −3 for moderately inferior (probable influence on diagnosis), and −4 for markedly inferior (impairing diagnosis). Scores could be used more than once if reconstructions were judged to be equivalent (16).

Quantitative Analysis

Three-dimensional spherical regions of interest (ROIs) were drawn on each reconstruction by using GE Advantage Workstation software 3.2 (GE Healthcare). The reconstructions were linked in each viewport so that identical ROIs could be drawn in the same location on each reconstruction. Three ROIs were drawn in the liver, one within each psoas muscle, two in the subcutaneous abdominal fat (one anterior and one posterior), and within the single largest hepatic metastasis fulfilling the study criteria per patient. Care was taken to avoid confounding structures such as large vessels, lesions, and atheromatous plaques in each ROI.

For each reconstruction, the contrast-to-noise ratio (CNR) relative to muscle was calculated for the liver as $(ROI_{liver} - ROI_{m})/SD$, where ROI_{liver} is the mean attenuation (in Hounsfield units) for the liver and ROI_{m} is the mean attenuation of the psoas muscles. The CNR for hepatic metastases was also calculated as $(ROI_{liver} - ROI_{metastasis})/SD$, where SD is the mean image noise based on subcutaneous fat using the average standard deviation in Hounsfield units (32).

Statistical Analysis

Summary statistics of series score, series rank, and CNR were provided as means, standard deviations, and ranges by sequence and dose (SD vs RD). Lesion detection and diagnosis status were summarized by using frequencies and percentages by dose. The McNemar test was used to compare SD and RD scans with respect to diagnostic accuracy. κ Statistics were estimated for lesion detection to assess reader agreements. If any reader detected a lesion for SD or RD, then that lesion was considered detected for that dose when compared against the consensus reference standard. This approach assesses the visibility of a lesion between scans while limiting the effects of reader differences. If any reader classified a lesion as malignant, that lesion was considered malignant for that SD or RD scan when compared against the consensus reference standard. Per-participant performance was not calculated because lesion-level assessment best delineates the comparison between scans. Rank and CNR of sequences and dose were estimated and compared by using a linear mixed model where participant and reader were included as random effects. The odds ratio of having a lesion confidence score of 4 or 5 and an artifact score of 1 or 2 was calculated by using a generalized estimating equations approach to account for the random effect of each reader. Tukey-Kramer adjustment was used to control overall type I error rate at 5%. All tests were two sided, and *P* values of .05 or lower were considered to indicate statistically significant differences. Statistical analysis was performed by using SAS, version 9.4 (SAS Institute, Cary, NC).

Results

Participant Characteristics

The studied group of 51 participants consisted of 29 men and 22 women, with a mean age of 57 years ± 13 (standard deviation) (range, 23–85 years), an average weight of 81 kg ± 16 (range, 51–131 kg), and a mean body mass index of 28 kg/m^2 ± 5 (range, 18–41 kg/m^2).

Participants underwent robust oncologic imaging protocols during therapy, with 49 out of 51 participants having more than 10 cross-sectional studies for comparison review. The most recent CT examination for comparison to the study CT examination was performed within a mean period of 83 days ± 28 (range, 48–196 days). Within a period of 6 months before or after the study examination, three CT scans ± 1 (range, one to six scans) were performed and available as comparisons. Of the two patients who underwent only one examination during this 6-month period, one had undergone 10 CT examinations and the other had undergone 15 CT examinations for comparison beyond that 6-month period. Additionally, every participant had undergone other examinations (eg, PET/CT and MRI) to varying degrees, and these examinations were useful in the characterization of liver lesions.

Radiation Dose

For SD examinations, the mean $CTDI_{vol}$ was 25.8 mGy ± 7.9 (range, 19.2–46.7 mGy), the mean SSDE was 30.7 mGy ± 5.8 (range, 24.3–46.8 mGy), and the mean DLP was 714.6 mGy·cm ± 250.2 (range, 407.1–1420.1 mGy·cm). The mean dose reduction of the RD scan was 53.9% ± 3.7

Table 2: False-Positive Lesion Localizations by Reader during SD FBP and RD ASIR-V 60 Evaluations

Lesion Size and Reader No. or Result	SD FBP			RD ASIR-V 60		
	No. of Lesions Diagnosed as Malignant	No. of False-Positive Lesions	False-Positive Rate	No. of Lesions Diagnosed as Malignant	No. of False-Positive Lesions	False-Positive Rate
<0.6 cm						
1	55	7	12.7 (5.3, 24.5)	27	4	14.8 (4.2, 33.7)
2	52	11	21.2 (11.1, 34.7)	38	7	18.4 (7.7, 34.3)
3	63	12	19.1 (10.2, 30.9)	38	6	15.8 (6.0, 31.3)
At least one reader positive	75	17	22.7 (13.8, 33.8)	53	10	18.9 (9.4, 32.0)
At least two readers positive	57	10	17.5 (8.7, 29.9)	34	5	14.7 (5.0, 31.1)
0.6–1.0 cm						
1	106	5	4.7 (1.5, 10.7)	88	3	3.4 (0.7, 9.6)
2	102	5	4.9 (1.6, 11.1)	79	4	5.1 (1.4, 12.5)
3	106	4	3.8 (1.0, 9.4)	89	4	4.5 (1.2, 11.1)
At least one reader positive	116	6	5.2 (1.9, 10.9)	98	5	5.1 (1.7, 11.5)
At least two readers positive	109	5	4.6 (1.5, 10.4)	88	4	4.6 (1.3, 11.2)
>1.0 cm						
1	51	1	2.0 (0.0, 10.4)	47	1	2.1 (0.1, 11.3)
2	50	2	4.0 (0.5, 13.7)	48	1	2.1 (0.1, 11.1)
3	50	2	4.0 (0.5, 13.7)	48	2	4.2 (0.5, 14.3)
At least one reader positive	52	2	3.8 (0.5, 13.2)	51	2	3.9 (0.5, 13.5)
At least two readers positive	51	2	3.9 (0.5, 13.5)	49	2	4.1 (0.5, 14.0)

Note.—Data in parentheses are 95% confidence intervals. ASIR-V 60 = adaptive statistical iterative reconstruction–V 60%, FBP = filtered back projection, RD = reduced dose, SD = standard dose.

(range, 50.0%–59.7%) with a mean $CTDI_{vol}$ of 11.8 mGy ± 3.3 (range, 9.6–21.2 mGy), mean SSDE of 14.1 mGy ± 2.4 (range, 11.9–21.0 mGy), and a mean DLP of 324.9 mGy·cm ± 104.6 (range, 203.1–637.1 mGy·cm).

Lesion Detection

Of the 260 lesions detected at reference standard assessment (233 metastatic; 27 benign), 212 (82%; 95% confidence interval [CI]: 76%, 86%) were detected with RD, while 252 lesions (97%; 95% CI: 94%, 99%) were detected with SD ($P < .001$). The per-lesion sensitivity for the SD FBP scan versus that of the RD ASIR-V 60 scan according to lesion size was as follows: 81% (95% CI: 69%, 89%; 58 of 72 lesions) versus 60% (95% CI: 48%, 71%; 43 of 72 lesions) for lesions smaller than 0.6 cm ($P = .001$), 99% (95% CI: 95%, 100%; 111 of 112 lesions) versus 84% (95% CI: 76%, 90%; 94 of 112 lesions) for lesions between 0.6 and 1.0 cm ($P < .001$), 100% (95% CI: 93%, 100%; 49 of 49 lesions) versus 98% (95% CI: 89%, 100%; 48 of 49 lesions) for lesions larger than 1.0 cm, and 94% (95% CI: 90%, 96%; 218 of 233 lesions) versus 79% (95% CI: 74%, 84%; 185 of 233 lesions) for all lesions. Performance data based on lesion size categories are listed in Table 2. Five participants were found to have no lesions that fulfilled the study criteria, and four participants were excluded from lesion detection data because they had more than 20 hepatic lesions. The other 42 participants had a median of four lesions (range, 1–20 lesions; 25th–75th percentile, 2–12 lesions) with a mean size of 0.7 cm ± 0.4 (range, 0.2–1.5 cm; 25th–75th percentile, 0.5–1.0 cm). The estimated κ for reader agreement of lesion detection was 0.35 for SD FBP and 0.65 for RD ASIR-V 60; agreement was higher for the RD studies given that readers consistently missed the same lesions. Readers 1, 2, and 3 correctly detected 87%, 76%, and 84% of lesions with SD FBP and 70%, 63%, and 66% with RD ASIR-V 60; the mean lesion confidence scores were 3.9 ± 1.4, 4.0 ± 1.6, and 4.4 ± 1.3 for SD FBP and 3.2 ± 1.7, 3.3 ± 1.8, and 3.7 ± 1.8 for RD AV60, respectively. Readers reported significantly fewer lesion confidence scores of 4 or 5 for RD AV60 than for SD FBP (odds ratio [OR], 0.49; 95% CI: 0.40, 0.60; $P < .001$).

Qualitative Image Assessment

The mean image quality scores for SD FBP and RD ASIR-V 60 for readers 1, 2, and 3 were 2.0 ± 0.5, 1.2 ± 0.6, 2.0 ± 0.7 and 2.9 ± 0.8, 2.5 ± 0.7, and 3.1 ± 0.9, respectively. Readers reported significantly fewer image quality scores of 1 or 2 for RD AV60 than for SD FBP (OR, 0.07; 95% CI: 0.04, 0.13; $P < .001$). In order of highest to lowest, side-by-side ranking of overall image quality was as follows (Fig 2): SD AV60 (mean, −0.6 ± 0.7), SD AV30 (mean, −0.7 ± 0.7), SD A80 (mean, −0.9 ± 0.7), SD FBP (mean, −1.0 ± 0.8), RD AV60 (mean, −1.5 ± 0.8), RD AV30 (mean, −1.6 ± 0.9), RD A80 (mean, −1.8 ± 0.8), and RD Veo 3.0 (mean, −2.0 ± 1.0). The image quality estimated mean rank was significantly different ($P < .001$) as a function of SD versus RD: SD scans had an estimated mean of −0.1 (95% CI: −1.0, −0.7), and RD scans had an estimated mean of −1.8 (95% CI: −1.9,−1.6]). The image quality estimated mean rank was also significantly different when comparing between each

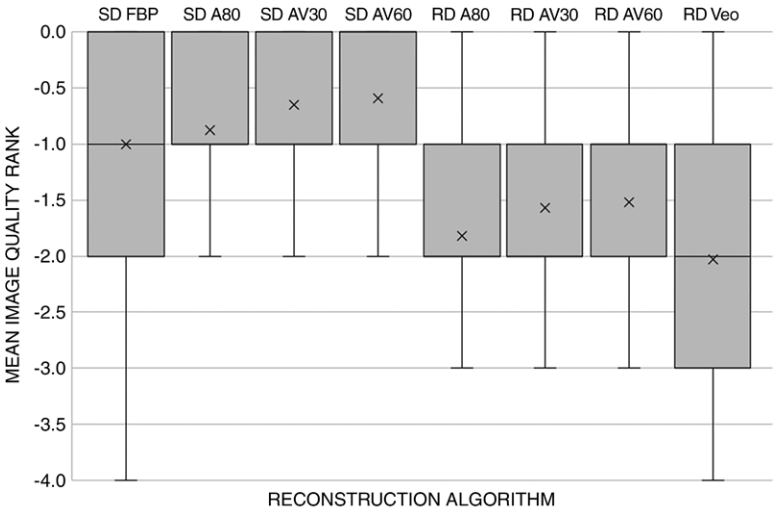

Figure 2: Graph shows results of qualitative image evaluation of overall image quality rank. A score of 0 was given for the best series, −1 for slightly inferior (no influence on diagnosis), −2 for mildly inferior (possible influence on diagnosis), −3 for moderately inferior (probable influence on diagnosis), and −4 for markedly inferior (impairing diagnosis). Mean image quality rank was significantly different from the next best reconstruction except between the standard dose *(SD)* and reduced dose *(RD)* adaptive statistical iterative reconstruction AV60/AV30 reconstructions (*P* = .89) and the SD filtered back projection *(FBP)*/SD A80 reconstructions (*P* = .57). *A80* = adaptive statistical iterative reconstruction (ASIR) 80%, *AV30/60* = ASIR-V 30%/60%.

reconstruction ($P < .001$): AV60 had a mean of −1.1 (95% CI: −1.2, −0.9); AV30, a mean of −1.1 (95% CI: −1.3, −1.0); A80, a mean of −1.4 (95% CI: −1.5, −1.2); FBP, a mean of −1.5 (95% CI: −1.6, −1.3); and Veo 3.0, a mean of −1.6 (95% CI: −1.7, −1.4). Pairwise comparisons also revealed statistically significant differences between radiation dose and reconstruction algorithm, with the exception of FBP to A80 (*P* = .57) and AV30 to AV60 (*P* = .89).

Quantitative Image Assessment

Estimated mean CNR in the liver was significantly different ($P < .001$) as a function of SD versus RD: SD scans had a mean CNR of 5.7 (95% CI: 4.9, 6.8), and RD scans had a mean CNR of 4.1 (95% CI: 3.5, 4.8). With the exception of A80 to Veo 3.0 (*P* = .97), the estimated mean CNR in the liver was also significantly different when comparing between each reconstruction (removing the effect of dose level); it was 6.0 (95% CI: 5.1, 7.0) for AV60, 4.8 (95% CI: 4.1, 5.7) for AV30, 5.3 (95% CI: 4.5, 6.2) for A80, 3.4 (95% CI: 2.9, 4.0) for FBP, and 5.2 (95% CI: 4.4, 6.2) for Veo 3.0 (Table 3).

Discussion

Our prospective evaluation demonstrated that performance at reduced radiation dose (mean $CTDI_{vol}$, 11.8 mGy) with ASIR-V is inferior to that for standard radiation dose FBP (mean $CTDI_{vol}$, 25.8 mGy) for subcentimeter hepatic lesion evaluation in colorectal cancer with lower detection rates, per lesion sensitivity and reader confidence. Previous studies of FBP, ASIR, ASIR-V, and Veo 3.0 had shown AV30%–60% to provide the best balance of qualitative and quantitative performance. While our current data indicate that these reconstructions could not maintain observer performance at reduced radiation doses for low contrast low attenuation (LCLA) liver lesion assessment, qualitative evaluation does suggest that IRs offer improved perceptual image quality when comparing within each dose level (14,19).

Target radiation dose reduction of 50% in our study was chosen to approximate the 25th–75th percentile $CTDI_{vol}$ reported by sites in the Dose Index Registry of the American College of Radiology for contrast-enhanced CT of the chest, abdomen, and pelvis ($CTDI_{vol}$, 9–19 mGy) (31). Additionally, this modest radiation dose reduction, compared with prior studies, was chosen because inferior hepatic lesion detection and characterization has been reported at doses below these levels (11,33). Goenka et al (34) had shown maintained performance at lower dose levels ($CTDI_{vol}$, 10.1 mGy) than ours, albeit with lower reader confidence; however, the reference SD in their liver lesion phantom study ($CTDI_{vol}$, 13.52 mGy) was significantly lower than the SD used in our current study ($CTDI_{vol}$, 25.8 mGy). With a similar reference dose level ($CTDI_{vol}$, 14.5 mGy), Pooler et al (11) prospectively showed that an RD of 5 mGy was inferior for LCLA liver lesion detection. In the study by Fletcher et al (27), baseline liver imaging radiation doses (mean, 24 mGy; range, 12.7–46.9 mGy) were in line with our mean $CTDI_{vol}$ of 25.8 mGy in an overweight study population (mean body mass index, 28.27 kg/m^2). Fletcher et al reported noninferiority for the detection of malignant hepatic lesions using 39% artificial dose reduction by noise insertion to an approximate $CTDI_{vol}$ of 14.6 mGy. However, in that study, just 18 of the nodules measuring less than 1 cm in size were malignant, and these lesions were of multiple different cancer types (27).

The detection of subtle pathologic findings, such as LCLA liver lesions in potentially resectable colorectal carcinoma, can markedly alter patient treatment. The identification of each liver metastasis is necessary not only to determine whether a patient is a surgical candidate but also to potentially direct other therapeutic decisions such as targeted therapies (35,36). Low contrast resolution is a function of lesion characteristics (size, relative attenuation to background), scanning technique (radiation dose level, collimation), reconstruction method (FBP vs IR algorithm, section thickness), and display (window width/level) (34). Our study showed that a significant number of lesions were either not identified or were mischaracterized on the RD scans (Table 2, Fig 3). Furthermore, readers demonstrated a significant loss in confidence when attempting to characterize lesions on the RD scan. Importantly, the inferior observer performance by RD scans in our study raises concern as to what proper dose levels should be used, particularly in oncologic imaging. The RD scans in our study were performed at dose levels considered to be standard in some prior studies (11,34). On the basis of our study results and our experience in practice, we propose that observer

Table 3: Attenuation, Noise, and CNR in the Abdomen according to Dose and Reconstruction Method

Parameter	SD FBP	SD ASIR 80	RD Veo 3.0	SD ASIR-V 30	SD ASIR-V 60	RD ASIR 80	RD ASIR-V 30	RD ASIR-V 60
Attenuation (HU)*								
Liver	121 ± 22	121 ± 22	115 ± 20	121 ± 22	121 ± 22	117 ± 21	117 ± 21	117 ± 21
Psoas muscle	64 ± 7	64 ± 7	63 ± 8	64 ± 7	64 ± 7	65 ± 8	64 ± 8	65 ± 8
Metastases†	64 ± 20	64 ± 20	63 ± 20	64 ± 20	64 ± 20	63 ± 20	63 ± 20	63 ± 20
Noise in subcutaneous fat‡	13 ± 2	8 ± 2	11 ± 2	9 ± 1	8 ± 1	11 ± 2	12 ± 2	9 ± 1
CNR§								
Liver	4.6 ± 2.0	7.2 ± 3.5	5.1 ± 2.2	6.5 ± 2.8	8.0 ± 3.4	5.2 ± 2.6	4.6 ± 2.1	5.8 ± 2.7
Metastases	4.3 ± 2.7	7.0 ± 4.5	5.2 ± 2.5	6.1 ± 3.7	7.5 ± 4.6	4.9 ± 3.3	4.4 ± 2.8	5.6 ± 3.5

Note.—Data are means ± standard deviations. ASIR = adaptive statistical iterative reconstruction, CNR = contrast-to-noise ratio, FBP = filtered back projection, RD = reduced dose, SD = standard dose. Numbers after the reconstruction method are the reconstruction percentage.

* No significant difference in attenuation was identified between reconstructions.

† The attenuation of the single largest lesion that fulfilled study criteria was measured in each participant.

‡ Noise = Hounsfield unit standard deviation.

§ CNR was significantly different from the next-best reconstruction except between RD ASIR 80 and RD Veo 3.0 (P = .97). CNRs ranked from highest to lowest are as follows: SD ASIR-V 60, SD ASIR 80, SD ASIR-V 30, RD ASIR-V 60, RD ASIR 80, RD Veo 3.0, RD ASIR-V 30, and SD FBP.

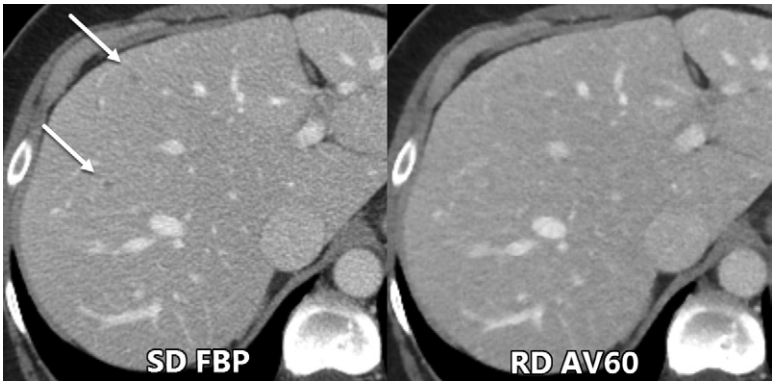

Figure 3: Axial contrast-enhanced CT images show example of two small low-contrast liver metastases (arrows) that were seen by all three readers during the evaluation of standard radiation dose *(SD)* filtered back projection *(FBP)* images but were missed during the evaluation of reduced dose *(RD)* adaptive statistical iterative reconstruction–V 60% *(AV60)* images.

performance for small LCLA liver lesions cannot be adequately maintained much below our dose levels. Although Fletcher et al (27) showed maintained performance for LCLA liver lesion detection at 14.6 mGy, their study used artificial noise insertion, different image reconstruction methods, and heterogeneous hepatic lesion etiologies and the study population weight/body mass index was unreported. Further observer studies with lesser radiation dose reduction such as with a $CTDI_{vol}$ of 15–20 mGy, assuming an overweight population, are needed to determine proper dose levels. Objective measures such as a detectability index as reported by Smith et al (9) would be useful in determining achievable dose levels incorporating in vivo noise texture, image resolution, and the task function.

These more objective and clinically relevant assessments are critical in the current imaging environment where IR methods that are complex due to vendor differences and blended combinations may be difficult to translate to practice. While dramatic de-noising can be carried out with IR techniques, there are potential degradations of related noise texture, contrast, and resolution in resultant CT images (37,38). It is now understood that spatial resolution can vary with nonlinear IR techniques depending on the underlying object contrast (39,40). It is therefore not surprising that the standard assessment of image noise and CNR do not necessarily correlate with improved performance (28). As seen in our study, RD AV60 had a mean CNR of 5.82, yet demonstrated reduced performance compared with SD FBP, which had a lower mean CNR of 4.58.

CNR assessment of all eight reconstructions revealed an expected correlation between the reconstruction methods, as published by Goodenberger et al (14) with SD AV60 having the highest mean CNR of 8.0. Interestingly, while the utility of IR is typically discussed as it relates to radiation dose reduction, our study suggests that readers derive benefit from IR even at standard doses (Figs 2, 4), albeit not enough to overcome an approximately 50% radiation dose reduction. Goodenberger et al had previously shown that FBP was inferior to IR methods at the lower mean $CTDI_{vol}$ of 6.8 mGy ± 3.8. Our study further confirms this relationship, but now at higher dose levels, with SD FBP inferior qualitatively when compared with SD AV30 and SD AV60. While the mean image quality rank trended higher for SD A80 compared with SD FBP, this was not significant (P = .57). In line with the prior Goodenberger et al study, lower qualitative performance was shown with Veo 3.0 compared with A80, AV30, and AV60 in the current study. Even with a slightly higher CNR compared with SD FBP, RD Veo 3.0 was ranked significantly lower qualitatively, which further supports CNR to be an inadequate surrogate marker of observer performance.

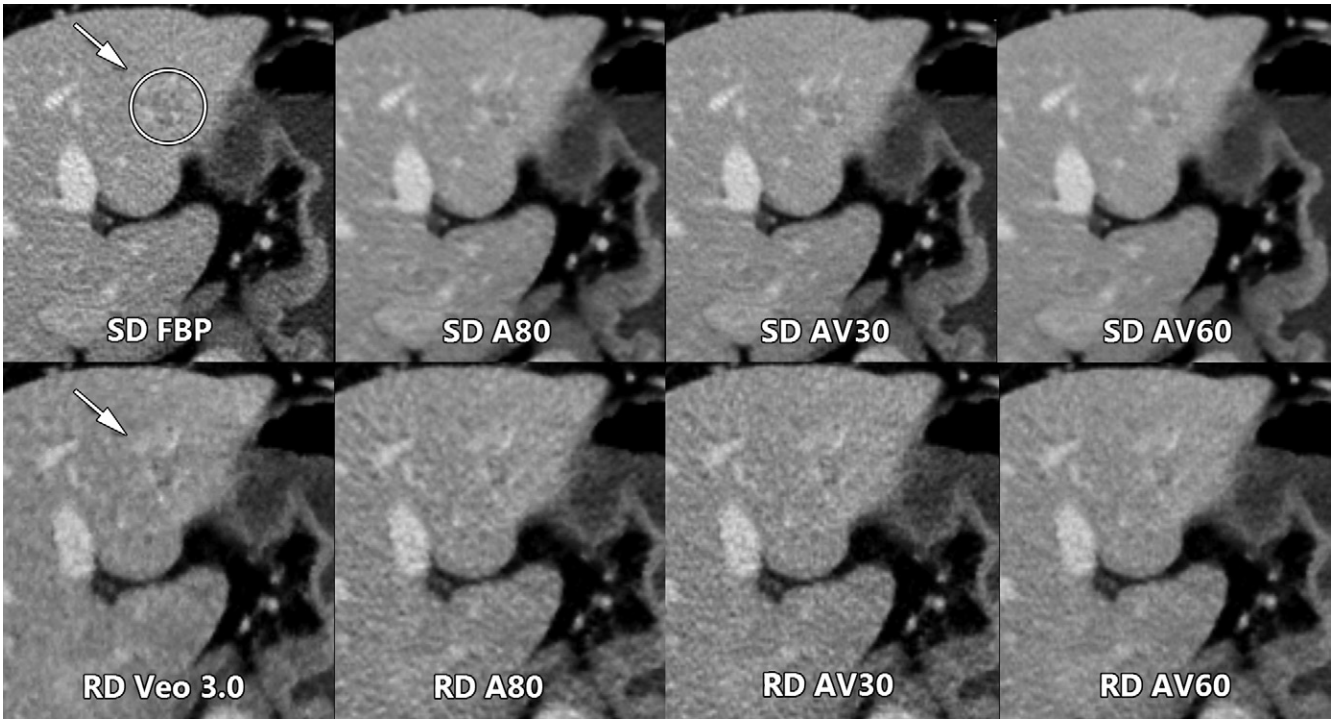

Figure 4: Axial contrast-enhanced CT images of the abdomen show qualitative comparison of a low-contrast left hepatic metastasis (arrow and circle, arrow) between standard radiation dose *(SD)* and reduced dose *(RD)* scans obtained in the same breath hold during the current study. Readers ranked the AV60 reconstruction highest in their respective SD and RD scan groups. *FBP* = filtered back projection, *A80* = adaptive statistical iterative reconstruction (ASIR) 80%, *AV30* = ASIR-V 30%, *AV60* = ASIR-V 60%.

Our lesion detection and sensitivity data support prior study results where IR algorithms were unable to maintain image quality with progressively increasing degrees of radiation dose reduction (33). For RD primary lesion assessment, we used AV60, which was a superior algorithm in prior studies when compared with FBP, ASIR, and Veo 3.0 (14,19). Just as RD AV60 could not maintain image quality at a 54% dose reduction in our study, the same has been seen with other IR methods (24,41). However, it is important to note that this observation in our study occurred at a higher standard reference dose level than most prior relevant studies. The combined results of multiple prior studies appear to suggest 10 mGy to be a mean dose level below which liver lesion detection is at risk for reduced performance (10,11,40), but even this dose level was found to be inadequate in the evaluation of LCLA small liver lesions in our current study. The authors' experience in a tertiary oncologic center suggests that relatively higher radiation doses are still needed for the consistent detection and characterization of small LCLA liver lesions, particularly in patients that may undergo surgical resection of hepatic metastases. Importantly, the range of required radiation doses not only depends on the clinical task, contrast agent injection parameters, and patient factors such as size, but also on the equipment in use at each center. The utility of operating at reduced radiation dose levels that may not reach a diagnostic threshold for the clinical task is in question, particularly in populations where the degree of radiation exposure is of unlikely significance (42).

There were several limitations of this study. First, direct objective measurement of lesion detection was performed at only two radiation dose levels. However, effort was made to choose levels that would provide additional information in the literature. For example, our SD provides insight into imaging performance at our tertiary oncology center, which attempts to identify minute lesions that can alter treatment for patients with cancer. Furthermore, our RD scans allow comparison to the American College of Radiology dose index standard doses. Both the SD and RD scans provide new prospectively acquired information on observer performance at higher relative dose levels. Second, our assessment of SD/RD A80, SD/RD AV30, SD AV60, and RD Veo 3.0 was performed in a side-by-side manner without primary lesion detection evaluation. Our primary evaluation of SD FBP versus RD AV60 was chosen based on comparing the best reconstruction from Goodenberger et al (AV 60) and a standard evaluation without IR (FBP) at SD. Third, our quantitative evaluation included only CNR, mainly as a validation step given prior in-depth assessments such as recent work by Euler et al, which included ASIR-V (14,28). Fourth, while each participant had biopsy-proven colorectal adenocarcinoma, the characterization of hepatic lesions in the reference standard was based on imaging diagnosis. Of note, given the extensive number of comparison examinations performed before and after the study examination for each participant, creation of the reference standard based on consensus was robust and consistent with earlier studies. Further evaluation of CT lesion detection in this setting in combination with MRI using a hepatobiliary contrast agent would be of interest,

particularly if the studied group may undergo hepatic resection. The reference standard bias in our study using predominate comparison to CT likely overestimates performance. Fifth, our study population was specifically selected for participants of a single cancer type with already suspected hepatic metastases. While this allowed for a robust evaluation of hepatic lesion detection in colorectal carcinoma, observer performance may not translate to other patient groups and cancers. Additionally, further evaluation with a larger number of participants and observers is needed to confirm and expand upon our findings. Last, our results do not directly correlate to other vendors or body regions.

In summary, our prospective study indicates that CT evaluation of small low-contrast liver lesions is compromised in the setting of modest radiation dose reduction and that iterative reconstructions could not maintain observer performance. However, qualitative evaluation does suggest that iterative reconstructions offer improved perceptual image quality when comparing within each dose level. If the clinical task requires the detection of small low-contrast liver lesions, radiation dose levels should be maintained, at levels that may be higher than those listed in the American College of Radiology dose index registry. Further research is necessary to determine how these findings may correlate to other scanner platforms, CT manufacturers, dose levels, and reconstruction methods.

Acknowledgment: We thank our Scientific Publications group for assistance in editing our manuscript.

Author contributions: Guarantors of integrity of entire study, C.T.J., L.N.V.; study concepts/study design or data acquisition or data analysis/interpretation, all authors; manuscript drafting or manuscript revision for important intellectual content, all authors; manuscript final version approval, all authors; agrees to ensure any questions related to the work are appropriately resolved, all authors; literature research, C.T.J., N.A.W., L.N.V., Y.C., E.S.; clinical studies, C.T.J., N.A.W., L.N.V., X.L., B.R.; experimental studies, L.N.V., X.L., B.R., E.S., S.G.; statistical analysis, C.T.J., L.N.V., W.W., E.S., S.G.; and manuscript editing, C.T.J., N.A.W., L.N.V., B.R., Y.C., E.S., S.G.

Disclosures of Conflicts of Interest: **C.T.J.** disclosed no relevant relationships. **N.A.W.** disclosed no relevant relationships. **L.N.V.** disclosed no relevant relationships. **X.L.** disclosed no relevant relationships. **B.R.** disclosed no relevant relationships. **D.M.** disclosed no relevant relationships. **W.W.** disclosed no relevant relationships. **Y.C.** disclosed no relevant relationships. **E.S.** Activities related to the present article: disclosed no relevant relationships. Activities not related to the present article: is a member of the advisory board of Imalogix; has given expert testimony for Rubin Anders; institution has grants or grants pending with GE, Siemens, and Bracco; institution has patents (planned, pending, or issued) with GE and Imalogix; institution receives royalties from GE, Imalogix, 12Sigma, and Gammex. Other relationships: disclosed no relevant relationships. **S.G.** disclosed no relevant relationships.

References

1. Eisenhauer EA, Therasse P, Bogaerts J, et al. New response evaluation criteria in solid tumours: revised RECIST guideline (version 1.1). Eur J Cancer 2009;45(2):228–247.
2. Levin DC, Rao VM, Parker L. The recent downturn in utilization of CT: the start of a new trend? J Am Coll Radiol 2012;9(11):795–798.
3. Moreno CC, Hemingway J, Johnson AC, Hughes DR, Mittal PK, Duszak R Jr. Changing abdominal imaging utilization patterns: perspectives from medicare beneficiaries over two decades. J Am Coll Radiol 2016;13(8):894–903.
4. Sagara Y, Hara AK, Pavlicek W, Silva AC, Paden RG, Wu Q. Abdominal CT: comparison of low-dose CT with adaptive statistical iterative reconstruction and routine-dose CT with filtered back projection in 53 patients. AJR Am J Roentgenol 2010;195(3):713–719.
5. Nelson RC, Feuerlein S, Boll DT. New iterative reconstruction techniques for cardiovascular computed tomography: how do they work, and what are the advantages and disadvantages? J Cardiovasc Comput Tomogr 2011;5(5):286–292.
6. Patino M, Fuentes JM, Singh S, Hahn PF, Sahani DV. Iterative reconstruction techniques in abdominopelvic CT: technical concepts and clinical implementation. AJR Am J Roentgenol 2015;205(1):W19–W31.
7. Flicek KT, Hara AK, Silva AC, Wu Q, Peter MB, Johnson CD. Reducing the radiation dose for CT colonography using adaptive statistical iterative reconstruction: a pilot study. AJR Am J Roentgenol 2010;195(1):126–131.
8. Singh S, Kalra MK, Hsieh J, et al. Abdominal CT: comparison of adaptive statistical iterative and filtered back projection reconstruction techniques. Radiology 2010;257(2):373–383.
9. Smith TB, Solomon J, Samei E. Estimating detectability index *in vivo*: development and validation of an automated methodology. J Med Imaging (Bellingham) 2018;5(3):031403.
10. Solomon J, Marin D, Roy Choudhury K, Patel B, Samei E. Effect of radiation dose reduction and reconstruction algorithm on image noise, contrast, resolution, and detectability of subtle hypoattenuating liver lesions at multidetector CT: filtered back projection versus a commercial model-based iterative reconstruction algorithm. Radiology 2017;284(3):777–787.
11. Pooler BD, Lubner MG, Kim DH, et al. Prospective evaluation of reduced dose computed tomography for the detection of low-contrast liver lesions: direct comparison with concurrent standard dose imaging. Eur Radiol 2017;27(5):2055–2066.
12. Ehman EC, Yu L, Manduca A, et al. Methods for clinical evaluation of noise reduction techniques in abdominopelvic CT. RadioGraphics 2014;34(4):849–862.
13. Pickhardt PJ, Lubner MG, Kim DH, et al. Abdominal CT with model-based iterative reconstruction (MBIR): initial results of a prospective trial comparing ultralow-dose with standard-dose imaging. AJR Am J Roentgenol 2012;199(6):1266–1274.
14. Goodenberger MH, Wagner-Bartak NA, Gupta S, et al. Computed tomography image quality evaluation of a new iterative reconstruction algorithm in the abdomen (adaptive statistical iterative reconstruction-V) a comparison with model-based iterative reconstruction, adaptive statistical iterative reconstruction, and filtered back projection reconstructions. J Comput Assist Tomogr 2018;42(2):184–190.
15. Telesmanich ME, Jensen CT, Enriquez JL, et al. Third version of vendor-specific model-based iterative reconstruction (Veo 3.0): evaluation of CT image quality in the abdomen using new noise reduction presets and varied slice optimization. Br J Radiol 2017;90(1077):20170188.
16. Jensen CT, Telesmanich ME, Wagner-Bartak NA, et al. Evaluation of abdominal computed tomography image quality using a new version of vendor-specific model-based iterative reconstruction. J Comput Assist Tomogr 2017;41(1):67–74.
17. Shuman WP, Green DE, Busey JM, et al. Model-based iterative reconstruction versus adaptive statistical iterative reconstruction and filtered back projection in liver 64-MDCT: focal lesion detection, lesion conspicuity, and image noise. AJR Am J Roentgenol 2013;200(5):1071–1076.
18. Fan JYM, Melnyk R. Benefits of AsiR-V reconstruction for reducing patient radiation dose and preserving diagnostic quality in CT exams. White paper, GE Healthcare. 2014.
19. Lee S, Kwon H, Cho J. The detection of focal liver lesions using abdominal CT: a comparison of image quality between adaptive statistical iterative reconstruction V and adaptive statistical iterative reconstruction. Acad Radiol 2016;23(12):1532–1538.
20. Lim K, Kwon H, Cho J, et al. Initial phantom study comparing image quality in computed tomography using adaptive statistical iterative reconstruction and new adaptive statistical iterative reconstruction v. J Comput Assist Tomogr 2015;39(3):443–448.
21. Kwon H, Cho J, Oh J, et al. The adaptive statistical iterative reconstruction-V technique for radiation dose reduction in abdominal CT: comparison with the adaptive statistical iterative reconstruction technique. Br J Radiol 2015;88(1054):20150463.
22. Volders D, Bols A, Haspeslagh M, Coenegrachts K. Model-based iterative reconstruction and adaptive statistical iterative reconstruction techniques in abdominal CT: comparison of image quality in the detection of colorectal liver metastases. Radiology 2013;269(2):469–474.
23. Vardhanabhuti V, Riordan RD, Mitchell GR, Hyde C, Roobottom CA. Image comparative assessment using iterative reconstructions: clinical comparison of low-dose abdominal/pelvic computed tomography between adaptive statistical, model-based iterative reconstructions and traditional filtered back projection in 65 patients. Invest Radiol 2014;49(4):209–216.

24. Baker ME, Dong F, Primak A, et al. Contrast-to-noise ratio and low-contrast object resolution on full- and low-dose MDCT: SAFIRE versus filtered back projection in a low-contrast object phantom and in the liver. AJR Am J Roentgenol 2012;199(1):8–18.
25. Dobeli KL, Lewis SJ, Meikle SR, Thiele DL, Brennan PC. Noise-reducing algorithms do not necessarily provide superior dose ptimization for hepatic lesion detection with multidetector CT. Br J Radiol 2013;86(1023):20120500.
26. Schindera ST, Odedra D, Raza SA, et al. Iterative reconstruction algorithm for CT: can radiation dose be decreased while low-contrast detectability is preserved? Radiology 2013;269(2):511–518.
27. Fletcher JG, Yu L, Li Z, et al. Observer performance in the detection and classification of malignant hepatic nodules and masses with CT image-space denoising and iterative reconstruction. Radiology 2015;276(2):465–478.
28. Euler A, Solomon J, Marin D, Nelson RC, Samei E. A third-generation adaptive statistical iterative reconstruction technique: phantom study of image noise, spatial resolution, lesion detectability, and dose reduction potential. AJR Am J Roentgenol 2018;210(6):1301–1308.
29. Brady SL, Kaufman RA. Investigation of American Association of Physicists in Medicine Report 204 size-specific dose estimates for pediatric CT implementation. Radiology 2012;265(3):832–840.
30. Boone J SK, Cody D, et al. Size-specific dose estimates (SSDE) in pediatric and adult body CT examinations: report ofAAPMtask group 204. American Association of Physicists in Medicine website. 2011.
31. Kanal KM, Butler PF, Sengupta D, Bhargavan-Chatfield M, Coombs LP, Morin RL. U.S. Diagnostic Reference Levels and Achievable Doses for 10 Adult CT Examinations. Radiology 2017;284(1):120–133.
32. Marin D, Nelson RC, Schindera ST, et al. Low-tube-voltage, high-tube-current multidetector abdominal CT: improved image quality and decreased radiation dose with adaptive statistical iterative reconstruction algorithm—initial clinical experience. Radiology 2010;254(1):145–153.
33. Schindera ST, Winklehner A, Alkadhi H, et al. Effect of automatic tube voltage selection on image quality and radiation dose in abdominal CT angiography of various body sizes: a phantom study. Clin Radiol 2013; 68(2):e79–e86.
34. Goenka AH, Herts BR, Obuchowski NA, et al. Effect of reduced radiation exposure and iterative reconstruction on detection of low-contrast low-attenuation lesions in an anthropomorphic liver phantom: an 18-reader study. Radiology 2014;272(1):154–163.
35. Abdalla EK, Vauthey JN, Ellis LM, et al. Recurrence and outcomes following hepatic resection, radiofrequency ablation, and combined resection/ablation for colorectal liver metastases. Ann Surg 2004;239(6):818–825; discussion 825–827.
36. Choti MA, Sitzmann JV, Tiburi MF, et al. Trends in long-term survival following liver resection for hepatic colorectal metastases. Ann Surg 2002;235(6):759–766.
37. Hernandez-Giron I, Geleijns J, Calzado A, Veldkamp WJ. Automated assessment of low contrast sensitivity for CT systems using a model observer. Med Phys 2011;38(Suppl 1):S25–S35.
38. Chen B, Ramirez Giraldo JC, Solomon J, Samei E. Evaluating iterative reconstruction performance in computed tomography. Med Phys 2014;41(12):121913.
39. Chen B, Christianson O, Wilson JM, Samei E. Assessment of volumetric noise and resolution performance for linear and nonlinear CT reconstruction methods. Med Phys 2014;41(7):071909.
40. Jensen K, Andersen HK, Smedby Ö, et al. Quantitative measurements versus receiver operating characteristics and visual grading regression in CT images reconstructed with iterative reconstruction: a phantom study. Acad Radiol 2018;25(4):509–518.
41. Solomon J, Wilson J, Samei E. Characteristic image quality of a third generation dual-source MDCT scanner: Noise, resolution, and detectability. Med Phys 2015;42(8):4941–4953.
42. Brenner DJ, Shuryak I, Einstein AJ. Impact of reduced patient life expectancy on potential cancer risks from radiologic imaging. Radiology 2011;261(1):193–198.